



The Impact of the El-Niño Southern Oscillation Precipitation and the Surface Temperature over the Upper Blue Nile Region

Firew Molla^{1,2*}, Abebe Kebede^{1,3} and U. Jaya Prakash Raju¹

¹*Department of Physics, Washera Geospace and Radar Science Laboratory, Science College, Bahir Dar University, Bahir Dar, Ethiopia.*

²*Department of Physics, Oda Bultum University, Ethiopia.*

³*Institute of Meteorology and Hydrology, Arba Minch University, Ethiopia.*

Authors' contributions

This work was carried out in collaboration between all authors. All authors read and approved the final manuscript.

Article Information

DOI: 10.9734/JSRR/2018/45657

Editor(s):

(1) Dr. Angela Gorgoglione, Department of Civil and Environmental Engineering, University of California, Davis, USA.

Reviewers:

(1) Bharat Raj Singh, Dr. APJ Abdul Kalam Technical University, India.

(2) Eric S. Hall, USA.

Complete Peer review History: <http://www.sciencedomain.org/review-history/28121>

Original Research Article

Received 20 September 2018

Accepted 07 December 2018

Published 04 January 2019

ABSTRACT

Precipitation is a climatic variable influenced by global weather parameter like, sea surface temperature from Pacific Ocean. Its effect in turn has an impact on crop production and other precipitation related results (add reference). In this research work, we have studied the impact of the El Niño-Southern Oscillation (ENSO) on surface temperature and precipitation over selected regions of Upper Blue Nile. We applied Pearson correlation analysis on the precipitation and sea surface temperature above the parts of Upper Blue Nile with monthly Climate Hazards Group InfraRed Precipitation with Station data (CHIRPS) anomaly and from four ENSO regions over the Equatorial Pacific Ocean. We have found that the Niño 4 region is a better matching region for the selected location of the Upper Blue Nile out of the four ENSO regions in the equatorial Pacific Ocean. Moreover, the Niño 4 region shows a negative correlation with precipitation and a positive correlation with temperature over Upper Blue Nile. Further evaluations of the relationships between precipitation and temperature with Niño 4 including the Atlantic oscillation, were conducted. Precipitation and temperature are partially correlated with Niño 4 and the Atlantic oscillation

*Corresponding author: E-mail: komeabekome@gmail.com;

however, precipitation was limited to a few months. The seasonal dependence of precipitation and temperature on the strength of El Niño and La Niña events in the Niño 4 region were evaluated over the Upper Blue Nile. Results show the temperature is maximum over the Upper Blue Nile region during the El Niño period and reverses for the La Niña events. Precipitation is reduced during the El Niño period and increases during the La Niña period.

Keywords: ENSO; precipitation; temperature and seasons.

1. INTRODUCTION

Precipitation is a climatic variable, which is influenced by global signals, like, sea surface temperature from the Pacific Ocean, and its effect, in turn, has an impact on crop production and other results in Ethiopia [1]. Extreme precipitation in Ethiopia has led to extensive food shortages as well as economic and climate lapses [2]. Such problems led to research to find the causes that influence precipitation to be extreme for a given region. The main source of variability in food production is the temporal and spatial fluctuations of rainfall [3]. This spatial variation of rainfall is largely controlled by altitude variation and temperature variation over the Pacific, Indian, and Atlantic Oceans [1]. The influence of these Oceans, especially, Pacific Ocean was studied at different locations in Ethiopia like the Upper Blue Nile with respect to discharge and drought conditions [4].

The climate of the Upper Blue Nile basin is divided into different seasons. Summer (kirmet) is a season where the maximum annual rainfall occurs in the region [5]. But the dry season has deficiency of rainfall in the region and small rainfall during spring (Belg). Rainfall and temperature vary considerably with topography in the upper Blue Nile River basin [6]. As the altitude increases, rainfall increases and temperature decreases. There are also other factors which cause variation in rainfall is the relationship between the ocean and the atmosphere [7]. In the previous century, attempts were made to understand the relationship between the ocean and the atmosphere globally and in different regions [8]. Climate variation is determined by hydrometeorology data such as rainfall, air and water temperature [9]. A correlation analysis has been made between sea surface temperature variation and regional weather and climatic variations [10]. One of the well-known independent variable is the El Niño Southern Oscillation (ENSO) which is a temperature gradient along the equatorial Pacific Ocean [11]. ENSO events exist in the Pacific Ocean. They

affect regions away from Pacific Ocean [12]. The El Niño Southern Oscillation (ENSO) is an event which involves fluctuating ocean temperatures in the central and eastern equatorial Pacific, coupled with changes in the atmosphere [12].

Around the world, several meteorologists have tried to determine patterns and the relationships between ENSO event and climate variables [13]. Among those meteorologists, Gilbert Walker was the one who determined the patterns of the ENSO [14]. The ENSO events generally classified into two types: La Niña which is caused by cold Ocean temperature and El Niño which is warm ocean temperature in the equatorial Pacific region [15]. The western portion of the equatorial Pacific Ocean is warmer compared with the eastern portion [16]. Occasionally, a small change in usual sea surface temperature pattern produces disruption of the wind along equator [14]. These sea surface temperature deviations from the normal alter ocean processes and impact global weather and climate [17]. The barometric pressure in the Pacific Ocean is higher in the east and lower in the west, but the pressure field can be changed [18]. This 'sea-saw' variation of the pressure field between the eastern and western parts of Pacific Ocean is called the Southern Oscillation [19]. Acting together with the oceanic and the atmospheric variations, this phenomenon is known as the El Niño-Southern Oscillation (ENSO) [20].

The Atlantic and near Atlantic region shows concurrent climate variability in a defined time scale [21]. This concurrent variation in ocean temperature, air temperature, rainfall, and surface pressure have a great influence on the socio-economic and land structure in the region [22]. The most prominent climatic variability in the region is the North Atlantic Oscillation (NAO), has a huge impact on regional and continental climates, especially in the Northern Hemisphere [23]. The North Atlantic Oscillation and its linkage with other regional patterns causes climate variability [23]. The region becomes colder and dryer than in normal situations [24]. The net movement of in the North Atlantic during the

winter time, which attracts warmer surface air, contains moisture which is distributed into most of Europe and further into regions of Asia [25]. The various influences of cooling and warming are observed in the Mediterranean, Northern Africa and the Middle East, and North America [26].

In this study, surface temperature and precipitation were evaluated due to the El Niño effect over the Upper Blue Nile. The intent was to understand the impact of the ENSO on the meteorological variables over parts of the Upper Blue Nile and to explain the time lag between ENSO in the different locations of the Upper Blue Nile depending on their climatic conditions. In addition, we studied the relationship between the North and South Atlantic sea surface temperature anomaly, precipitation, and temperature over the Upper Blue Nile, considering the effect of the ENSO in the Equatorial Pacific Ocean particularly the Niño 4 region, in order to understand the individual influence of the climatology of the study area.

Since El Niño affects most parts of the country, the current work focuses on surface temperature and rainfall variation for the Upper Blue Nile due to El Niño and the Atlantic sea surface temperature anomaly. The large scales

connection to the Blue Nile River Basin of Ethiopia results a change in basin rainfall and the Blue Nile water flow [27]. The El Niño Southern Oscillation index (ENSO) is a factor in the Upper Blue Nile Basin rainfall which is associated with both high and low rainfall in the region [4].

2. STUDY AREA

The Upper Blue Nile basin is locally called Abay, in the north-western part of Ethiopia (Fig 2.1). The topography of the basin is comprised of highlands and hills in the north-eastern part, is dominated by valleys in the southern and western parts [5]. The elevation varies from 480 m near the Sudanese/Ethiopian border to over 4200 m near the central part of the basin [28]. Ten weather stations located in various parts of the Upper Blue Nile were selected in different climatic regions to evaluate the effect of El Niño. The climate of the basin is tropical highland monsoonal, with the majority of the rain falling from June to October [5].

The climate in the basin varies considerably between the Ethiopian highlands and its confluence with the White Nile in Khartoum [6]. The spatial and temporal variation is affected by the movement of air masses associated with Inter Tropical Convergence Zone (ITCZ) [29].

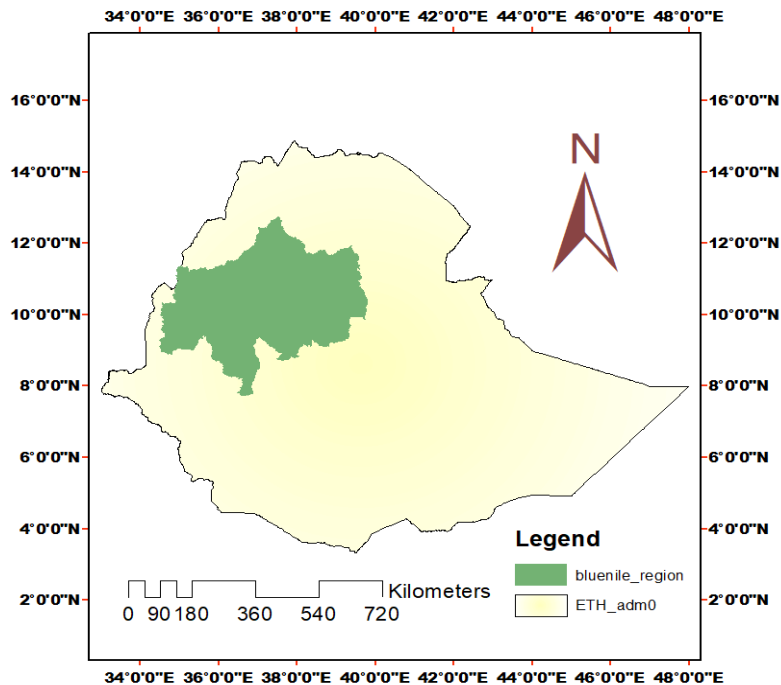


Fig. 2.1. Location of the upper Blue Nile basin and Ethiopia

During the winter dry season (known in Ethiopia as bega) the ITCZ lies south of Ethiopia and the Blue Nile region is affected by a dry northeast continental air-mass [29]. In March, the ITCZ returns, bringing small rains (known in Ethiopia as the belg) particularly to the southern and south western parts of the basin [30]. In May, the northward movement of the ITCZ produces a short intermission before the main wet season (known in Ethiopia as the kremt) [30].

In June, the ITCZ moves further north, and the southwest airstream extends over the entire Ethiopian highlands to produce the main rainy season [5]. This is also the main rainy season in the Sudan, though being further north and at lower altitudes [31].

The average annual rainfall varies between 1400 and 1800 mm/year, ranging from an average of about 1000 mm/year near the Ethiopia–Sudan border to 1400 mm/year in the upper part of the basin, and more than 2000 mm/year in the parts Didessa and Beles sub basins [31]. In the Sudan, the rainfall drastically decreases from about 1000 mm/year near the border with Ethiopia to less than 200 mm/year at the junction with the White Nile in the city of Khartoum [32]. The rainfall trend was studied in the upper Blue Nile basin, and most of the results showed that, there was no significant trend in the seasonal and annual basin-wide average rainfall [5,33].

The annual mean potential evapotranspiration decreases with increasing elevation from 1845 mm to 924 mm [6]. In the Sudan, potential evaporation increases, and this produces a significant loss of Blue Nile water [6]. For instance, the Sennar region has a potential evaporation rate of 2,500 mm/year, but receives only 500 mm/year of rain [34]. The temperature in the basin varies with elevation [5]. The climate is generally temperate at the higher elevations and tropical at the lower elevations [6]. Traditional classifications of climate in the upper basin use elevation as a controlling factor and recognize three regions namely: the Kolla zone below 1800 m, with mean annual temperatures in the range 20-28°C, the Woina Dega zone between 1800-2400 m, with mean annual temperatures in the range 16-20°C and; the Dega zone above 2400 m with mean annual temperatures in the range 6-16°C [6]. Increasing trends in temperature have been reported at different weather stations in the Upper Blue Nile in Ethiopia [35]. The analysis of the period 1941–1996, shows an important piece of evidence of

warming in most parts of the Sudan, namely the central and southern regions [36].

3. DATA AND METHODOLOGY

3.1 Data Sources

In the equatorial Pacific Ocean, four Niño regions based on the Extended Reconstructed Sea Surface Temperature version 5 (ERSSTv5) dataset were considered for the ENSO index, and the data for the period of 1982 to 2016 from the Climate Prediction Centre of National Oceanic and Atmospheric Administration (NOAA) was used for sea surface temperature anomaly data: Niño 1+2 (0°-10° South) (90° West 80° West), Niño 3 (5° North 5° South)(150° West -90° West), Niño4 (5° North 5° South) (160° East 150° West) and Niño 3.4 (5° North 5° South)(170-120° West).

Monthly Sea Surface Temperature (SST) data for the North Atlantic Oscillation (NAO), the South Atlantic Ocean (SAO) were obtained from the National Weather Service, Climate Prediction Centre (<http://www.cpc.noaa.gov/data/indices/>; Accessed 21 October 2018) for the period from 1982-2016.

Due to limited availability of rain gauge data; we have chosen the CHIRPS data. The Climate Hazards group Infra-Red Precipitation with Stations Climate Hazards group Infra-Red Precipitation with Stations (CHIRPS) v4.0, gridded data sources for monthly precipitation with 0.05° spatial resolutions for the time period 1982-2016 was used. In addition to this monthly surface temperature data obtained from Climatic Research Unit's gridded data set (CRU TS3.1) was used. The monthly surface temperature data totals at 0.5° spatial resolutions for the period 1982 to 2016 was used.

3.2 Methodology

In this section we computed the monthly precipitation or ten selected locations and temperature anomalies over the Upper Blue Nile. We also analyzed different time steps for the CHIRPS precipitation data over the selected locations in the Upper Blue Nile. The time step precipitation anomaly for selected locations were correlated with a one-month time step anomaly for four Niño regions. We selected the best Niño region which had good correlation with precipitation for each selected location.

Subsequently, we use the selected Niño to further correlate with precipitation and temperature over the Upper Blue Nile. The sea surface temperature anomaly (SSTA) and precipitation anomaly was calculated by the general formula given below. This standardized monthly anomaly values are represented mathematically as shown in Equation 1;

$$a_{i,j} = \frac{X_{i,j} - M_j}{S_j} \quad (1)$$

Where, $a_{i,j}$ is the standardized anomaly value for the j^{th} month of the i^{th} year, $X_{i,j}$ is the observed value for the j^{th} month of the i^{th} year and, m_j and S_j are mean and standard deviation for j^{th} month respectively.

Correlation coefficients were computed between the monthly precipitation anomalies for each location, with the indices indicating different time lags. Pearson correlation analysis was used to determine the association between two variables. The limits of the correlation coefficient values are +1 and -1. Zero correlation value indicates that no relationship, exists between the two variables, while +1 (positive) and -1 (negative) imply a strong linear association. The correlation equation is expressed in Equation 2 as;

$$R = \frac{\sum(x_i - \bar{x})(y_i - \bar{y})}{\sqrt{\sum(x_i - \bar{x})^2} \sqrt{\sum(y_i - \bar{y})^2}} \quad (2)$$

Where r is the correlation coefficient between X and Y where the variables X represents the rainfall or temperature and Y represents the ENSO index.

Correlation and partial correlation was used to depict the relationship between the Atlantic sea surface temperature anomaly values and the El-Niño southern oscillation (ENSO) particularly Niño4 with precipitation and temperature over the study area.

Partial correlation coefficients are expressed in Equation 3 as:

$$r_{xy/z} = \frac{r_{xy} - r_{xz}r_{yz}}{\sqrt{(1-r_{xz}^2)(1-r_{yz}^2)}} \quad (3)$$

Where $r_{xy/z}$ is the partial correlation coefficient between x and y after controlling involvement of z variable, while r_{xy} , r_{xz} and r_{yz} are correlation.

Lag correlation coefficients were calculated between the ENSO index and precipitation anomalies. We have also done comparisons of mean of rainfall and temperature on the selected Niño region for the El Niño and La Niña for each month of season. We calculated the occurrences of the ENSO phases occurrence based on sea surface temperature anomaly values above +0.5°C and below -0.5°C for grouping of three months (a season) for five consecutive months (Climate Prediction Center [CPC] classification).

Before computing correlation coefficient from climatic signals and precipitation data, sea surface temperatures were calculated to standardize the anomaly for the selected months (May, June, July, August, September: (MJJAS)) of summer precipitation for the Upper Blue Nile and the months (May, June, July, August: (MJJA)) of summer sea surface temperature for Pacific Ocean particularly the Niño 4 region and Atlantic Ocean which includes the North Atlantic oscillation and South Atlantic. After anomaly calculations for each season, the correlation and partial correlation coefficients were calculated.

4. RESULTS AND DISCUSSION

The results illustrate the correlation between the CHIRPS precipitation and the surface temperature data with the ENSO for different regions (Niño 1+2, Niño 3, Niño 4 and Niño 3.4). The results of sea surface temperature (SST) anomaly from four Niño regions and the precipitation in the Upper Blue Nile shows a very small correlation with the monthly time steps of anomaly. This result requires a different approach to quantify the link between the ENSO event and precipitation from the selected locations in the Upper Blue Nile. These various anomaly calculations were applied on the precipitation data, at one, three, six, nine, and twelve months anomaly intervals for each study area in the Upper Blue Nile region. Each type of monthly anomaly precipitation is associated with SSTA in the Equatorial Pacific Ocean, which is observed that one, three, six, and nine -month time steps (intervals) of the anomaly. We learned that the twelve months anomaly precipitation for each selected location of the Upper Blue Nile matches best with the Niño4 region in the four regions, and this is presented in Table 4.1.

Based on the correlation values, we took one region (Niño 4) out of the four Niño regions from the Pacific Ocean that was in good agreement with the precipitation anomaly, which was

supported by the correlation coefficients of -0.17, -0.25, -0.24, -0.23,-0.44,-0.14,-0.39 and -0.23 respectively between the Niño4 and the CHIRPS precipitation anomaly from the following weather stations: Ambo, Bahir Dar, Dangila, Deber-birhin, Dejen Dessie, Debre-markos and Metu. However, two locations Combolcha and Fitch were better associated with Niño 3.4, and Niño 3 respectively. The correlations indicate that variation of sea surface temperature in Niño 1+2, Niño 3.4 and Niño 4 regions have influenced precipitation in the Upper Blue Nile, and comparatively speaking, the maximum impact comes from the Niño 4 region. Negative values indicate that the cause for the small amounts of precipitation occurring in the Upper Blue Nile may be due to sea surface temperatures in the Niño that due to intensified particularly in the Niño 4 region.

An assessment of different lag correlations from 1 to 6 months was calculated for each time step. The result indicates that the lag correlation values reduce when monthly anomaly type increases.

The correlations for 1, 2, 3, 4, 5, and 6 months were computed, and the result showed that at the beginning (1, 2, 3, and 4), the magnitude of the correlation values were large compared to the lag correlation at five and six months, with a gradually decreasing magnitude as the time lag increases, which is validated in previous study [37].

The correlation coefficients are presented in Tables 4.1. The result shows the associations between locations in the Upper Blue Nile and the Niño region of the Pacific Ocean, and the magnitude of relationship amongst the different

regions. But the maximum correlations are observed in the Niño4 region in the Pacific Ocean. Also, other Niño regions have contributed on a portion to the selected location Niño4. The ENSO index indicated a variation in the sea surface temperature in the eastern part of Pacific Ocean, which create precipitation changes over the region, and the amount of variation is dependent on the ENSO region, which provided a different contribution to the study region.

The association between the monthly precipitation and the temperature in the Upper Blue Nile, along with the monthly sea surface temperature anomaly of Niño 4 region over Equatorial Pacific Ocean were evaluated. The result of correlation between the SSTA of Niño 4 region, and the precipitation and temperature are -0.25 and 0.32 respectively. The correlation coefficient indicates that the sea surface temperature anomaly for the Niño 4 region is inversely related for to precipitation and directly related to the temperature over study area. As the sea surface temperature anomaly of the Niño 4 region are increased, the amount of precipitation in the Upper Blue Nile decreased, while temperature association (trend) is similar to the Niño 4 anomaly, and this result is consistent with the findings of the study of Ethiopian Highland summer rainfall using correlation analysis [33]. The Equatorial Pacific Ocean temperature was negatively correlated with the summer rainfall, and there was general agreement that the Pacific sea surface temperature and summer rainfall are negatively correlated [33,38]. In addition, the summer rainfall is largely influenced by the sea surface temperature variation from the equatorial east Pacific, which is associated with rainfall variation from normal and was studied by [39].

Table 4.1. Correlations value for the monthly precipitation anomaly and the ENSO index

Correlation values for weather Stations with index						
Location	Lat in degrees	Lon in degrees	Niño 1+2	Niño 3	Niño 3.4	Niño 4
Ambo	8.9847	37.83967	-0.12	-0.14	-0.13	-0.17
Bahir Dar	11.595	37.385	-0.1	-0.19	-0.24	-0.25
Dangila	11.434	36.846	-0.07	-0.16	-0.22	-0.24
Deberbirhin	9.6333	39.5	-0.15	-0.18	-0.2	-0.23
Dejen	10.171	38.15067	-0.25	-0.36	-0.41	-0.44
Dessie	11.12	39.63333	0	-0.05	-0.09	-0.14
Markos	10.326	37.7392	-0.23	-0.34	-0.38	-0.39
Metu	8.2833	35.56667	-0.07	-0.17	-0.22	-0.23
Fitch	9.7667	38.7333	-0.25	-0.27	-0.25	-0.24
Combolcha	11.084	39.71763	-0.10	-0.16	-0.17	-0.15

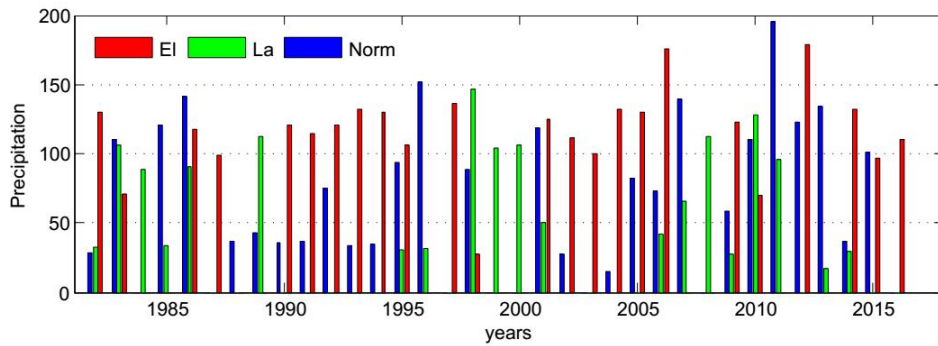


Fig. 4.1. The precipitation in the upper Blue Nile Region (1982–2016) and its association with El Niño and La Niña years. Red represents El Niño events, Green represents normal events and Black represents La Niña events

Fig. 4.1 shows the occurrences of El Niño, La Niña and normal precipitation events in the Upper Blue Nile region over 35 years. It can be shown from this figure, that the frequency of occurrence of an El Niño event has greater probability of occurrence than normal and La Niña events. However, the frequency occurrence of normal and La Niña are almost the same with various magnitude of precipitation over the Upper Blue Nile region during the given period. We conclude that an El Niño event is a dominant event for the period of 1982-2016 based on the frequency of occurrence and its association with precipitation. But normal and La Niña events occurred occasionally during the period of 1982-2016.

ENSO precipitation but the amount of precipitation increases in the La Niña years, with respect to normal ENSO precipitation. These effects are obvious in the summer and short rainy season, while in the dry season, there is a problem identifying the influence of ENSO events on precipitation using the precipitation versus season graph, and that may be due to precipitation amount. During the dry season the amount of precipitation is slightly above and below normal during the El Niño and La Niña seasons respectively.

Fig. 4.2 shows the variation of precipitation in the Upper Blue Nile region for 3-month averaged periods between 1982–2016 for three types (phases) of ENSO events. We determine from this figure, that the amount of precipitation is reduced in the El Niño years, relative to normal

Table 4.2. Frequency of normal, El Niño and La Niña events associated with precipitation over the Upper Blue Nile during the period 1982–2016

Event	Frequency
Normal	8
El Niño	19
La Niña	8

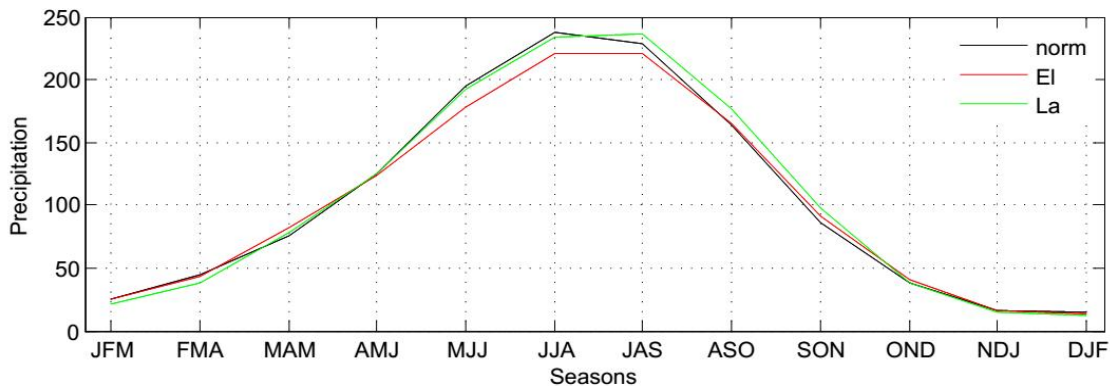


Fig. 4.2. Seasonal precipitation in the upper Blue Nile region averaged during El Niño, La Niña, and normal years

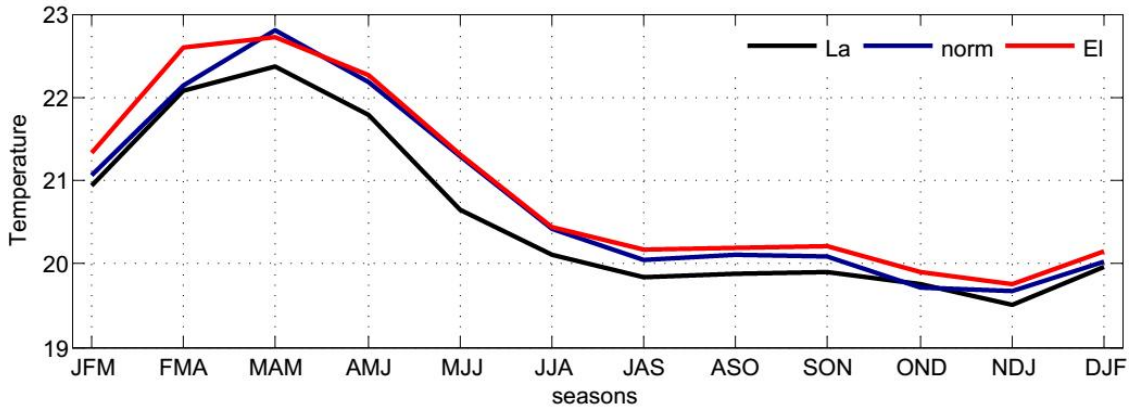


Fig. 4.3. Seasonal temperatures in the upper Blue Nile region averaged during El Niño, La Niña, and normal years

Fig. 4.3 indicates the seasonal temperature over in the Upper Blue Nile region averaged during 1982 – 2016 for three types of ENSO events. We can see from this figure, that seasonal temperature is maximum during the El Niño phase with respect to normal, while the minimum temperature occurred during La Niña phase. In addition, the magnitude of temperature deviation from normal is maximum in the La Niña phase as compared to the El Niño phase. Upper Blue Nile temperature becomes cooler than normal during formation of La Niña phase, which has small increase in temperature during El Niño phase.

The phase of ENSO events classified based on sea surface temperature anomaly values above +0.5°C anomaly with 5 consecutive overlapping 3-month periods for the El Niño event, while sea surface temperature anomaly values are below -0.5°C anomaly for La Niña events and represents the normal phase of ENSO (NOAA Operational Definitions for El Niño and La Niña). This phase classified further into weak, moderate

and strong events based on the threshold value for at least 3 consecutive overlapping 3-month periods. The threshold values of the strength of events are presented in Table 4.3.

Table 4.3. El Niño and La Niña episodes

Event	Category	Value
El Niño	Weak	0.5 - 0.9
El Niño	Moderate	1.0 - 1.4
El Niño	Strong	1.5 ≤
La Niña	Weak	-0.5 - -0.9
La Niña	Moderate	-1.0 - -1.4
La Niña	Strong	-1.5 ≥

The graph below shows that the precipitation pattern over the Upper Blue Nile region by ENSO events including the strength of event at different magnitudes for the region. The graphs that explain the influence of the ENSO phases (Normal, El Niño, and La Niña) over precipitation of Upper Blue Nile region are provided below.

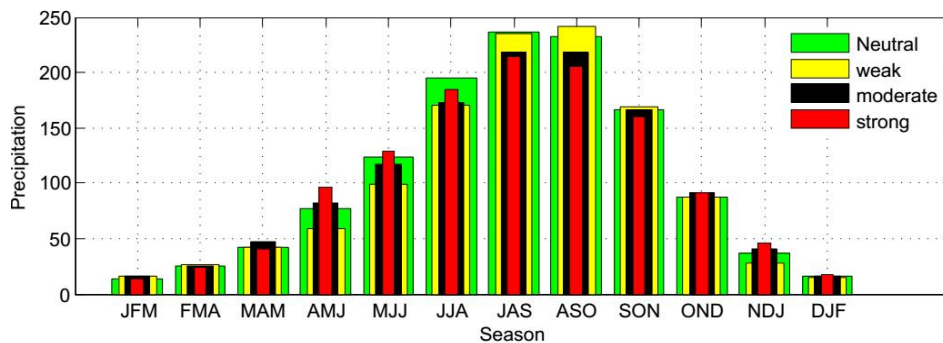


Fig. 4.4. (a) shows the comparison of precipitation between normal and El Niño years during 1982–2016 for the upper Blue Nile region

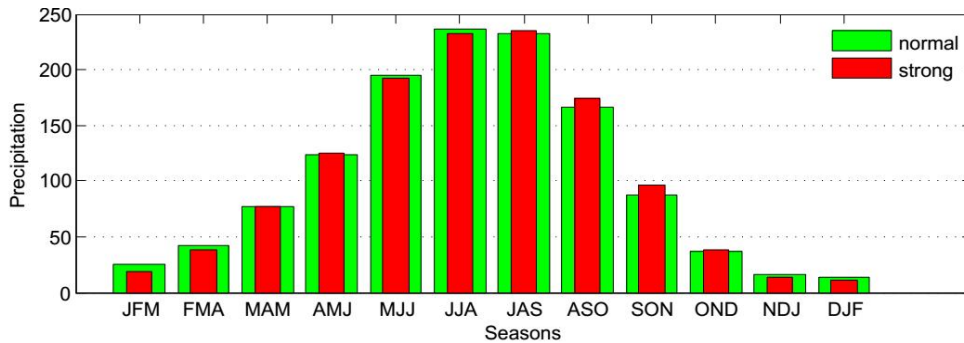


Fig. 4.4. (b) showed the comparison of precipitation between normal and strong La Niña years during 1982–2016 for the upper Blue Nile region

The relationships of normal year and El Niño year with precipitation at different strength are presented in Fig. 4.4 (a). In this figure, the amounts of precipitation are slightly lower than normal during the El Niño event during May, June, July (MJJ), June, July, August (JJA), and July, August, September (JAS). The seasonal precipitation varies with respect to normal, and below normal precipitation occurred during weak and moderate El Niño states, but above normal precipitation during strong El Niños during October, November, December (OND), March, April, May (MAM), and September, October, November (SON). Fig. 4.4 (a) these seasons do not include the long term rainfall (summer). Precipitation within weak and moderate El Niño events are the same as normal in the months of November, December, January (NDJ), but very small deviation above normal precipitation are observed during strong El Niño events. In months of December, January, February (DJF), precipitation is above normal in weak and moderate state of El Niño and almost the same during strong El Niño state on the graph shown in Fig. 4.4 (a).

In general, the seasonal precipitation in the Upper Blue Nile region is below normal during the El Niño season, which is supported by the results shown in Fig. 4.4 (a). The amount of precipitation is reduced when the strength of events is increased. The amount of reduction depends on the magnitude of the event (weak, moderate, or strong).

We also examined the association between strong La Niña and normal years with precipitation in the Upper Blue Nile, and the results are presented in Fig. 4.4(b). The reason that we only considered strong La Niña events is because there was fewer instances of weak and moderate La Niña event during 1982 - 2016. The

results show that above average and below average precipitation events seems to be equally observed in the Upper Blue Nile region. However, we calculated the deviation from normal by averaging all above and below normal precipitation and comparing them to determine the influence of the strong La Niña events, based on strength.

Our results are similar to the notion of El Niño being associated with below-average rainfall, while La Niña associated with above-average rainfall which is seen in [40]. Fig. 4.4 (b), the above and below average precipitation are almost equally observed, and this might be due to the relative strength and the start dates of La Niña events. The influence of starting dates of the La Niña seasons were noted with respect to flood, or extreme flood, and drought conditions, and when La Niña started, whether in April, May, June (AMJ), June, July, August (JJA), or July, August, September (JAS), when there is a maximum chance for flood or extreme flood to occur. But, when La Niña started late in August, September, October (ASO), there is was a very small chance floods as seen in [4].

The figure below shows the temperature deviation in the Upper Blue Nile region during El Niño and La Niña years.

The seasonal temperature increments and decrements in the Upper Blue Nile region were evaluated with respect to normal temperatures and the strength of El Niño events. The results are presented in Fig. 4.5(a). In Fig. 4.5(a) the seasonal temperature is maximum during February, March, April (FMA), March, April, May (MAM), and January, February, March (JFM) for all event strengths, except during the below normal temperatures in the season months of March, April, May (MAM) with moderate El Niño

event. In all El Niño cases, we observed that the rising temperatures tend to be warmer than normal during spring and winter. Other season temperatures are slightly warmer than normal with respect to the strength of El Niño events. Strong events have more influence on the seasonal temperatures, but below normal temperatures are observed during April, May, June (AMJ).

The temperature deviations during strong La Nina season are illustrated in Fig. 4.5(b) which show that all seasonal temperature are below normal except during July, August, September (JAS), and October, November, December (OND), when the temperature is above normal. However, the amount of temperature reduction is different amongst the season during the strong La Niña season. The temperature variation in the Upper Blue Nile region depend on the ENSO phase and the strength of events.

The impacts of the North and South Atlantic sea surface temperature anomaly on precipitation and temperature over the Upper Blue Nile are included in this study. Their correlation coefficients and partial correlation coefficient values are shown in Table 4.4. The maximum

correlation coefficient was obtained during May-August (May, June, July, August: MJJA) at the Niño 4 sea surface temperature in the Pacific Ocean, and with the May-September (May, June, July, August, September: MJJAS) precipitation in the Upper Blue Nile. Although, the partial correlation coefficient between the Niño 4 sea surface temperature and precipitation (by controlling for the North Atlantic oscillation) is slight different from the situation when not controlling for the North Atlantic oscillation, and the maximum difference occurred when controlling for both the North Atlantic and South Atlantic sea surface temperature anomaly, most of the temperature increment or decrement is due to the South Atlantic sea surface temperature anomaly. The partial correlation indicates that the South Atlantic sea surface temperature anomaly greatly contributes to summer precipitation in the Upper Blue Nile, and it can magnify the relationship between the Niño 4 in the Pacific Ocean and summer precipitation at Upper Blue Nile region. However, the associations between the South Atlantic Sea surface temperatures and seasonal precipitation when removing the effect of Niño 4 are less significant.

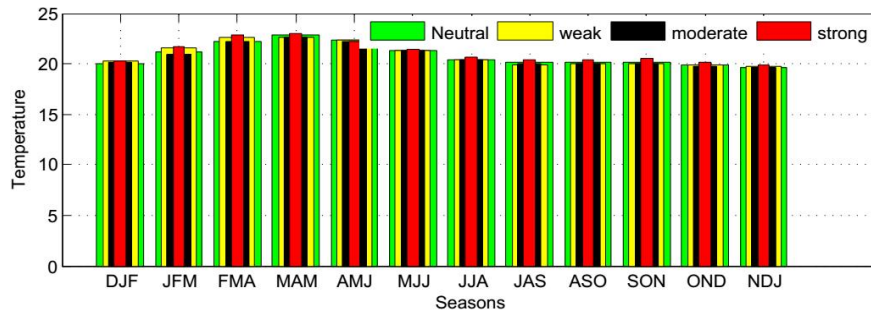


Fig. 4.5 (a) shows the comparison of temperature between normal and El Niño events during 1982 - 2016 in the upper Blue Nile region

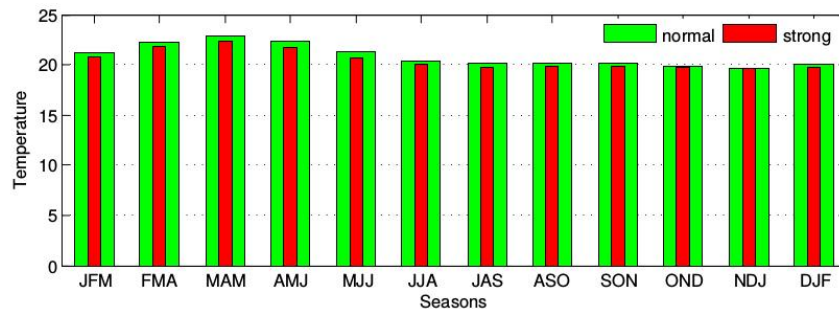


Fig. 4.5 (b) shows the comparison of temperature between normal and strong La Niña events during 1982–2016 in the upper Blue Nile region

Table 4.4. Correlation between the monthly anomaly and the May, June, July, August, September (MJJAS) precipitation and the May, June, July, August (MJJA)-Niño 4, North Atlantic Oscillation (NAO), and South Atlantic Oscillation (SAO) sea surface temperature anomaly

Correlation type	Considered variable	Correlation result
Correlation Coefficient	Niño 4 anomaly with precipitation anomaly	-0.548
	NAO anomaly with precipitation anomaly	0.359
	SAO anomaly with precipitation anomaly	0.373
Partial Correlation Coefficient	Niño 4 anomaly with precipitation anomaly controlling NAO	-0.526
	NAO anomaly with precipitation anomaly controlling Niño 4	0.316
	Niño 4 anomaly with precipitation anomaly controlling SAO	-0.457
	Niño 4 anomaly with precipitation anomaly controlling NAO and SAO	-0.456

We analyzed the link between the Upper Blue Nile temperature anomalies and climate signal (i.e., Niño 4, NAO, and SAO) anomalies using correlation and partial correlation analysis to compute the correlation coefficient. The correlation values for temperature in the Upper Blue Nile region and climatic signals, such as Niño 4, NAO and SAO are presented in Tables 4.5. As seen in Table 4.5 the maximum correlation value occurred between the NAO temperature anomaly in the Atlantic Ocean and temperature in the Upper Blue Nile. All partial correlation coefficients were associated with the Upper Blue Nile temperature, but relationships

are different, and tend to reduce the magnitude of the correlation values. The magnitude of the partial correlation values higher than correlation values.

Among different climate signals we found the NAO is strong positive correlation with the annual temperature of the Upper Blue Nile. The NAO and SAT indices show a positive correlation with precipitation and temperature, however, the Niño 4 has a negative correlation with annual precipitation and positive for temperature in the Upper Blue Nile.

Table 4.5. Correlation between monthly anomaly temperatures and Niño 4, North Atlantic, and south Atlantic Sea surface temperature anomaly

Correlation type	Variables considered	Correlation results
correlation coefficient	Niño 4, anomaly with temperature anomaly	0.329
	NAO anomaly with temperature anomaly	0.368
	SAO anomaly with temperature anomaly	0.10
partial correlation coefficient	Niño 4, anomaly with temperature anomaly controlling NAO	0.330
	NAO anomaly with temperature anomaly controlling Niño 4	0.370
	SAO anomaly with temperature anomaly controlling Niño 4,	0.148
	Niño 4, anomaly with temperature anomaly controlling NAO and SAO	0.336

Table 4.6. Annual correlation values of Niño 4 SST, North and South Atlantic Ocean temperature indices with precipitation and temperature index

Climate signal	Precipitation index	Temperature index
Niño 4 SST	-0.33	0.44
NAO SST	0.36	0.60
SAT SST	0.16	0.19

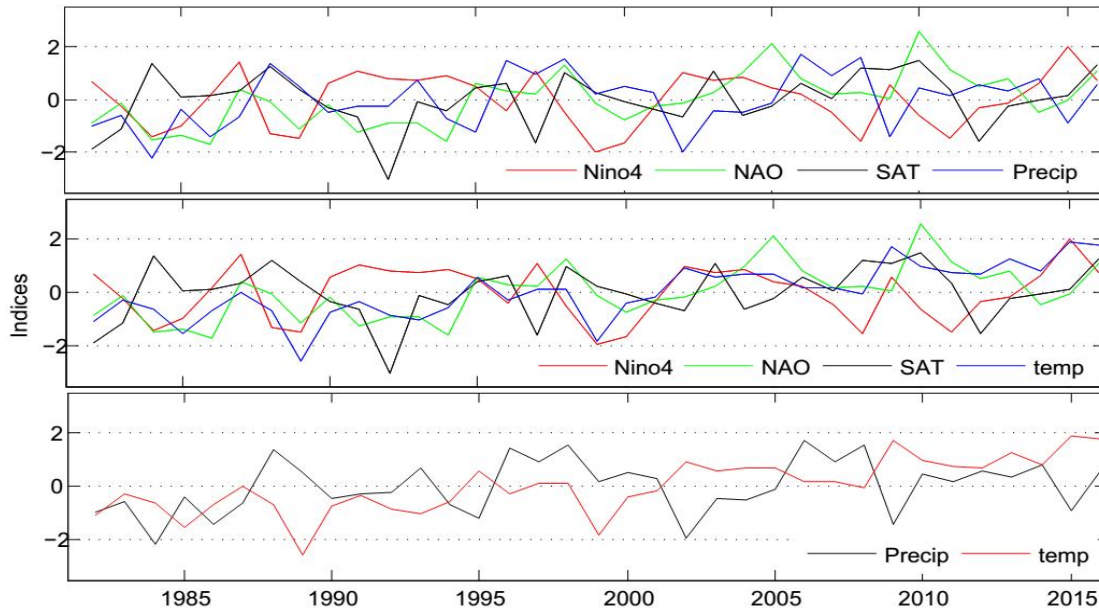


Fig. 4.6. Standardized annual precipitation and temperature variability over the upper Blue Nile and ENSO in Niño 4, North Atlantic Oscillation (NAO), South Atlantic Temperature (SAT), of and sea surface temperature indices for the time series for the period from 1982-2016

The top panel displays the association between Niño 4, NAO, and SAT with precipitation; the middle panel displays the association between Niño 4, NAO, and SAT with temperature in the Upper Blue Nile; the bottom panel displays the association between temperature and precipitation in the Upper Blue Nile.

There exists a time gap between the variation of Niño 4 and the response of the precipitation in the region because both indices reach the maximum deviation from mean at different times. Furthermore, the cold Niño 4 SST index in the Equatorial Pacific Ocean leads to wet conditions in the Upper Blue Nile region, and the inverse occurs for the warm Niño 4 SST index.

The North and South Atlantic temperature indices have a positive association with the precipitation index. Annual precipitation variation in the Upper Blue Nile region is influenced by the North and South Atlantic Ocean temperature and the annual correlation value is shown on the Table 4.6. We understand the weather condition of the Upper Blue Nile region, based on precipitation index, in terms of wet and dry years which are depicted on Fig. 4.6. Wet weather occurred in 1988, 1996, 1998, 2006, and 2008 while dry conditions existed nearly in 1984, 1986, 1995, 2002, 2009, and 2015. Based on the magnitude of events, the 1984 and 2002 events

resulted in extremely dry conditions. Also, we can identify that eleven wet and dry events, including five events in 1984, 1986, 1996, 1998, and 2006, that may be due to the NAO parallel variation of sea surface temperature, when the sea surface temperature of the NAO was reduced in 1984 and 1986 during the observed dry condition in the Upper Blue Nile region, and the ENSO and the Niño 4 decreased and increased respectively. However, the effect may be dominated by NAO. There are five events in 1988, 2002, 2008, 2009 and 2015 which may be due to the ENSO and Niño 4 SST variation. Figure 4.6 in the middle panel shows that the temperature variation in the Upper Blue Nile is greatly influenced by Niño 4 and the NAO SST index. Also, this influence is directly associated with temperature, which is supported by the annual correlation value shown in Table 4.6. However, the influence of the South Atlantic Ocean temperature index is weakly associated with temperature in the Upper Blue Nile region. Temperature is associated directly with ENSO in Niño 4, NAO and SAT as shown in Table 4.6.

The bottom panel indicates precipitation and temperature have opposite associations in the region of the Upper Blue Nile. The variation of ocean temperature from Pacific and Atlantic are the main cause for changing temperatures

and precipitation in the Upper Blue Nile region.

5. CONCLUSIONS

The impact of the El Niño–southern oscillation (ENSO) on precipitation in the Upper Blue Nile has been investigated, and is strongly linked with the Niño 4 region. The highest correlation coefficients observed from the SSTA in the Niño 4 region, with a precipitation anomaly in Dejen, DebreMarkos, and Bahir Dar are (-0.44, -0.39, and -0.25) respectively. In general, most of locations are negatively correlated with all Niño regions.

The association between precipitation and temperature in the Upper Blue Nile region with sea surface temperature in the Niño 4 region, has correlation values of -0.25 and 0.35 for precipitation and temperature respectively. Linear and partial correlation coefficients were computed from the Niño 4, NAO and SAT anomaly association with precipitation and temperature. The magnitudes of association were determined by considering strength of three ENSO phases. During El Niño events the amount of precipitation is reduced in the Upper Blue Nile region, and more reduction happens with strong as compared to weak and moderate El Niños, while the amounts of precipitation increase during strong La Niñas are comparable with normal events. The temperature is maximum in the Upper Blue Nile region during El Niño, and the highest temperature was observed in strong El Niño events compared to the weak and moderate El Niño events. La Niña events led to reduced temperatures that became cooler during the strong La Niña events.

The precipitation and temperature indicate opposite associations in region of the Upper Blue Nile. The variation of ocean temperature from Pacific and Atlantic is main cause for changing temperature and precipitation in the region.

ACKNOWLEDGMENT

The researchers would like to thank the Bahir Dar University for supporting this study to accomplish our research. We also like to say thank you very much for the physics department staffs by encouraging us to work further.

COMPETING INTERESTS

Authors have declared that no competing interests exist.

REFERENCES

1. Korecha D, Barnston AG. Predictability of June–September rainfall in Ethiopia. *Monthly Weather Review*. 2007;135(2): 628-650.
2. Low PS. ed. *Climate change and Africa*. Cambridge University Press; 2006.
3. Rosenzweig C, Iglesias A, Yang XB, Epstein PR, Chivian E. Climate change and extreme weather events; implications for food production, plant diseases, and pests. *Global Change and Human Health*. 2001;2(2):90-104.
4. Zaroug. Droughts and floods over the upper catchment of the Blue Nile and their connections to the timing of El Niño and La Niña events. *Hydrol. Earth Syst. Sci*. 2014; 18:1239–1249.
5. Conway D. The climate and hydrology of the Upper Blue Nile, Ethiopia. *The Geographical Journal*. 2000;166:49-62.
6. Conway D. A water balance model of the Upper Blue Nile in Ethiopia. *Hydrology. Sci. J*. 1997;42:265–286.
7. Deressa TT. Measuring the economic impact of climate change on Ethiopian agriculture: Ricardian approach. *The World Bank*; 2007.
8. Melesse, Dessalegne T. Characteristics of Monthly and Annual Rainfall of the Upper Blue Nile Basin. Addis Ababa, Ethiopia; 2008.
9. Wigley TM, Briffa KR, Jones PD. On the average value of correlated time series, with applications in dendroclimatology and hydrometeorology. *Journal of Climate and Applied Meteorology*. 1984;23(2):201-213.
10. Walker GT, Bliss EW. *World Weather V, Memories of the Royal Meteorological Society*. 1932;4:53–84.
11. Meyers G. Variation of Indonesian through flow and the El Niño-southern oscillation. *Journal of Geophysical Research: Oceans*. 1996;101(C5):12255-12263.
12. Collins M, An SI, Cai W, Ganachaud A, Guilyardi E, Jin FF, Jochum M, Lengaigne M, Power S, Timmermann A, Vecchi G. The impact of global warming on the tropical Pacific Ocean and El Niño. *Nature Geoscience*. 2010;3(6):391.

13. Kovats RS, Bouma MJ, Hajat S, Worrall E, Haines A. El Niño and health. *The Lancet*. 2003;362(9394):1481-1489.
14. Holton JR, Dmowska R. El Niño, La Niña, and the southern oscillation. Academic Press. 1989;46.
15. Kug JS, Jin FF, An SI. Two types of El Niño events: Cold tongue El Niño an warm pool El Niño. *Journal of Climate*. 2009; 22(6):1499-1515.
16. Chang CP, Zhang Y, Li T. Interannual and interdecadal variations of the East Asian summer monsoon and tropical Pacific SSTs. Part I: Roles of the subtropical ridge. *Journal of Climate*. 2000;13(24): 4310-4325.
17. Zelle H, Appeldoorn G, Burgers G, Oldenborgh GJ. The relationship between sea surface temperature and thermo cline depth in the eastern equatorial pacific. *Journal of Physical Oceanography*. 2004; 34:643-655.
18. Bjerknes J. A possible response of the atmospheric Hadley circulation to equatorial anomalies of ocean temperature. *Tellus*. 1966;18(4):820-829.
19. Ogallo LJ, JE J. Teleconnection between seasonal rainfall over East Africa and global sea surface temperature anomalies. *Journal of the Meteorological Society of Japan*. Ser.II. 1988;66(6):807-822.
20. Rasmusson EM. El Niño and variations in climate: Large-scale interactions between the ocean and the atmosphere over the tropical Pacific can dramatically affect weather patterns around the world. *American Scientist*. 1985;73(2):168-177.
21. Hurrell JW. Decadal trends in the North Atlantic oscillation: Regional temperatures and precipitation. *Science*. 1995; 269(5224):676-679.
22. Bates B, Kundzewicz Z, Wu S. Climate change and water. Intergovernmental Panel on Climate Change Secretariat; 2008.
23. Hurrell JW, Van Loon H. Decadal variations in climate associated with the North Atlantic oscillation. In *Climatic Change at High Elevation Sites*. Springer, Dordrecht. 1997;69-94.
24. Oliver JE. *Encyclopedia of world climatology*. Cornwall, Springer. 2008;854.
25. Pope VD, Gallani ML, Rowntree PR, Stratton RA. The impact of new physical parametrizations in the Hadley Centre climate model: HadAM3. *Climate Dynamics*. 2000;16(2-3):123-146.
26. Visbeck M, Cullen H, Krahmann G, Naik N. The north Atlantic oscillation: Past, present, and future. *Geophys. Res. Lett*. 2001;98:12876 –12877.
27. Kebede S, Travi Y, Alemayehu T, Marc V. Water balance of Lake Tana and its sensitivity to fluctuations in rainfall, Blue Nile basin, Ethiopia. *Journal of Hydrology*. 2006;316(1- 4):233-247.
28. Gebremicael TG, Mohamed YA, Betrie GD, van der Zaag P, Tenerife. Trend analysis of runoff and sediment fluxes in the upper Nile basin: A combined analysis of statistical tests, physically-based models and land use maps. *J. Hydrol*. 2013;482: 57–68.
29. Steenhuis TS, Collick AS, Easton ZM, Leggesse ES, Bayabil HK, White ED, Awulachew SB, Adgo E, Ahmed AA. Predicting discharge and sediment for the Abay (Blue Nile) with a simple model. *Hydrological Processes. An International Journal*. 2009;23(26):3728-3737.
30. Awulachew SB, McCartney M, Steenhuis TS, Ahmed AA. A review of hydrology, sediment and water resource use in the Blue Nile Basin. *IWMI*. 2009;131.
31. Awulachew SB, Mccartney M, Steenhuis TS, Ahmed AA. A review of hydrology, sediment and water resource use in the Blue Nile Basin. *International Water Management Institute Colombo, Sri Lanka, IWMI Working Paper 131*. 2008;87.
32. Gamachu D. Aspects of climate and water budget in Ethiopia. Addis Ababa, Ethiopia: Addis Ababa University Press. 1977;71.
33. Seleshi Y, Zanke U. Recent changes in rainfall and rainy days in Ethiopia. *Int. J. Climatol*. 2004;24:973–983.
34. Block PJ. Integrated management of the Blue Nile Basin in Ethiopia: Hydro power and irrigation modeling. Discussion Paper No. 00700, Washington, DC: International Food Policy Research Institute. 2007;25.
35. Tekleab S, Mohamed Y, Uhlen brook S. Hydro-climatic trends in the Abay/upper Blue Nile Basin, Ethiopia. *Phys. Chem. Earth, Elsevier Ltd*. 2013;61–62,32–42.
36. Elagib NA, Mansell G, Martin. Recent trends and anomalies in mean seasonal and annual temperatures over Sudan. *Journal of Arid Environments*. 2000;45: 263–288.
37. Degefu MA, David P. Rowell, Woldeamlak Bewket A. Teleconnections between Ethiopian rainfall variability and global SSTs: Observations and methods for

- model evaluation. Meteorol Atmos Phys. 2017;129:173–186.
38. Diro GT, Grimes DIF, Black E. Teleconnections between Ethiopian summer rainfall and sea surface temperature. Part I—observation and modeling. Clim Dyn. 2011a;37:103–119.
39. Eltahir EAB. El Niño and the natural variability in the flow of the Nile River. Water Resour. Res. 1996;32:131–137.
40. Abteu W, Melesse AM, Dessaiegne T. El Niño southern oscillation link to the Blue Nile River Basin hydrology. Hydrol. 2009; 23.

© 2018 Molla et al.; This is an Open Access article distributed under the terms of the Creative Commons Attribution License (<http://creativecommons.org/licenses/by/4.0>), which permits unrestricted use, distribution, and reproduction in any medium, provided the original work is properly cited.

Peer-review history:

The peer review history for this paper can be accessed here:
<http://www.sciencedomain.org/review-history/28121>